BIOCHEMISTRY
including biophysical chemistry & molecular biology

Article

pubs.acs.org/biochemistry

Domain Selection in Metallothionein 1A: Affinity-Controlled Mechanisms of Zinc Binding and Cadmium Exchange

Tyler B. J. Pinter, Gordon W. Irvine, and Martin J. Stillman*

Department of Chemistry, The University of Western Ontario, London, Ontario, Canada N6A 5B7

ABSTRACT: Mammalian metallothioneins (MTs) are small, metal binding proteins implicated in cellular metal ion homeostasis and heavy metal detoxification. Divalent, metal-saturated MTs form two distinct domains; the N-terminal β domain binds three metals using nine Cys residues, and the C-terminal α domain binds four metals with 11 Cys residues. Domain selection during zinc binding and cadmium exchange to human MT1A was examined using a series of competition reactions with mixtures of the isolated domain fragments. These experiments were conducted at two biologically significant pH conditions where MTs exist *in vivo*. Neither zinc binding nor cadmium exchange showed any significant degree of specificity or selectivity based on detailed analysis of electrospray ionization mass spectrometric and circular dichroic data. Under acidic conditions, zinc binding and cadmium exchange showed slight α domain selectivity because of the increased preference for cooperative clustering of the α domain. Modeling of the reactions showed that at both physiological (7.4) and acidic (5.8) pHs, zinc binding and cadmium exchanges occur essentially randomly between the two fragments. The metal binding affinity distributions between the domain fragments are comingled and not significantly separated as required for a domain specific mechanism. The models show rather that the order of the binding events follows the order of the binding affinities that are distributed across both domains and that this can be considered quantitatively by the K_F^{Cd}/K_F^{Zn} binding constant ratio for each metal bound.

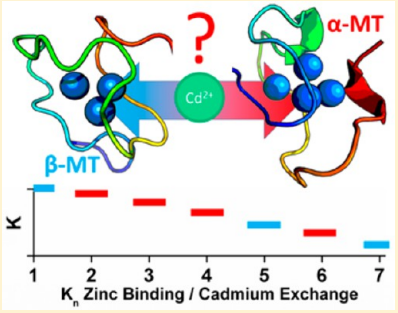

Zinc is intricately involved in a myriad of essential biological processes, including enzymatic catalysis, respiration, protein folding, cell signaling, and tissue growth.[1−3] These functions are significantly disrupted in the presence of cadmium from common sources of chronic cadmium exposure or, more rarely, acute cadmium poisoning.[4] The effect of cadmium toxicity on organisms has been well documented,[5] though the details of the toxicological action at the molecular level are not fully understood.[6,7] Cellular function is maintained only within a relatively narrow range of zinc concentrations,[8] and even low cadmium levels disrupt this.[9] The family of metallothionein proteins is considered to be largely responsible for maintaining the homeostatic control of zinc levels. It has been widely proposed that metallothionein is also involved in the detoxification of cadmium.[10] Currently, this detoxification mechanism is thought to occur in a domain selective fashion.[11]

Metallothioneins (MTs) are a superfamily of cysteine-rich, metal binding proteins that are found in all forms of life.[12,13] MTs bind biologically relevant metals with relatively high binding affinities (K_F). *In vivo* functions of MTs include metal homeostasis and detoxification of toxic metals, including cadmium.[14,15] MTs are generally characterized by their relatively small size (60−70 amino acids for human MTs) and high cysteine content, with up to one-third of the sequence comprised of Cys residues.[2] The redox properties of these thiols have also implicated MTs in the cellular response to oxidative stress.[16,17]

There are four known isoforms (and numerous subisoforms) of human metallothionein: MT1−MT4. The human MT1 and MT2 isoforms are involved in zinc homeostasis and heavy metal detoxification. MT3 and MT4 are expressed in specialized cells and tissue: MT3 in neuronal and glial brain cells and MT4 in squamous epithelial cells.[18] All human MT isoforms have a high degree of sequence conservation and, for the divalent metal saturated species, a two-domain metal cluster structure in which the domains are arranged in a dumbbell-like fashion.[19] It is important to note that structures have been determined only for the metal-saturated MTs, as the apo and partially metalated forms of MT are too fluxional, prohibiting nuclear magnetic resonance (NMR) structural analysis and preventing crystallization. Significantly, this two-domain cluster structure is formed only when MT is nominally saturated with seven divalent metals.[20]

The structure of the metal cluster is dependent on both the stoichiometry of added metals and the preferred coordination number of the metal(s).[21,22] For zinc- and cadmium-saturated human MT1A (Figure 1), the N-terminal β domain binds three metals using nine cysteine thiolates and the C-terminal α domain binds four metals using 11 cysteines; all of the metals are tetrahedrally coordinated through a combination of bridging and terminal thiolates (Figure 1B).[23] Past research has highlighted the significance of the metal-saturated, two-domain structure and its relevance to the metal binding and release properties. However, recent work by Chen et al.,[24] Krężel et al.,[25] and our group[26] has demonstrated the

Received: April 24, 2015
Revised: July 10, 2015
Published: July 13, 2015

DOI: 10.1021/acs.biochem.5b00452
Biochemistry 2015, 54, 5006−5016

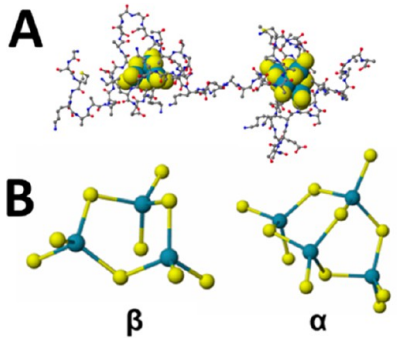

Figure 1. (A) Protein structure and (B) metalloclusters of the β and α domains of zinc-saturated rh-MT1A.

importance of intermediates in the metalation pathway from the metal-free apoMT to the fully metal-saturated holo-MT.

The mechanism for detoxification of cadmium by MT is currently reported to occur in a domain specific manner (Figure 2, pathway 2a).[27] This detoxification action can arise

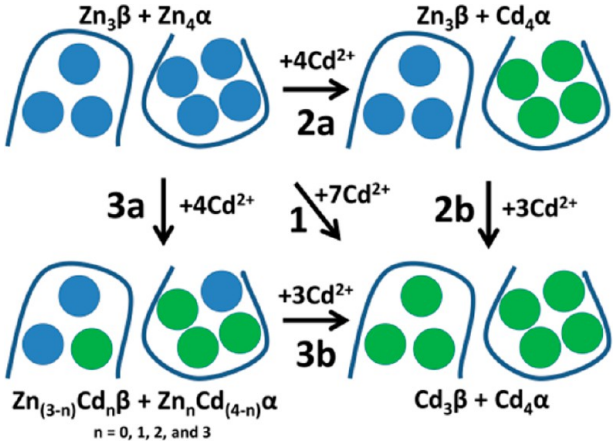

Figure 2. Possible metal exchange pathways for MT. The overall reaction is shown in pathway 1 with the substitution of seven Zn^{2+} ions (blue) for seven Cd^{2+} ions (green). A domain specific model in which the majority of the zinc is substituted in one of the domains first as shown in pathway 2 is employed. The random replacement model in which the metal exchange shows no significant metal preference between the domains and the metals are scrambled between the domains randomly as shown in pathway 3 is employed.

from the binding of Cd^{2+} by newly synthesized apo-MT or via exchange into Zn-saturated MT. This mechanism was proposed from analyses of cadmium exchange of Zn-MTs studied spectroscopically in which the domain specific exchange was used to explain the results that were thought to be related to equivalents of metals added and the "magic numbers" of MT metal binding.[22] However, spectroscopic methods used in the past provide the average metal loading of the protein. The use of ESI-MS to study cadmium−zinc replacement in the intact MT protein has been reported previously.[28]

Much of the current knowledge regarding domain specificity in MTs is based on results obtained from partial digestion of the MT strand (leaving one of the domains intact)[29] or the cadmium titrations of apo-MTs, studied by ^{113}Cd NMR.[30−32] Specifically, a pH dependence on the chemical shifts (and therefore the cadmium cluster formation) has been reported.[33] Significantly, these NMR studies report that binding of cadmium to the apoMT strand occurs cooperatively, with the first four added cadmium ions binding exclusively to the α domain, and that these are bound to the protein with the highest affinities.[34] Furthermore, it has been suggested that mixed Cd_4Zn_3-MT forms specifically Cd_4-α,Zn_3-β-MT in a highly domain selective manner.[32,35] Other NMR experiments have demonstrated metal exchange,[36] which is related to strand fluxionality.[37] Finally, the Cd_5Zn_2 X-ray crystal structure, obtained from the addition of cadmium to Zn_7MT, showed that the two remaining zinc ions were located in the β domain.[38]

The binding of metals to MT is largely an affinity-driven process. The distribution of metals within the full MT protein, between the two domains, as well as with competing MT strands, is reflected by those affinity constants ($K_{n,F}$, where n = 1−7); the higher-affinity sites will be saturated earlier.[39] Previous studies have demonstrated that there are multiple binding constants for zinc and cadmium, with an average binding constant difference of $>10^3$ (K_F),[40] and have shown mixed Cd,Zn-MT species form *in vitro* and *in vivo*.[11,36,41−43]

A domain specific model (Figure 2, pathway 2a followed by 2b) for cadmium displacement of zinc in Zn_7-MT would imply distorted binding affinity ratios (K_F^{Cd}/K_F^{Zn}) such that the α domain would have cadmium to zinc binding constant ratios all significantly higher than the β domain binding constant ratios to promote cadmium binding exclusively in the α domain. The random replacement model (Figure 2, pathway 3a followed by 3b) for this same reaction would involve a random ordering of binding affinity ratios or a set of binding affinity ratios close enough that the distribution would not dominate the distribution of metal in a specific domain.

In this paper, we report the fragment and domain preferences when zinc and cadmium bind to the isolated α and β fragments of MT1A. Detailed competition studies using ESI mass spectrometry and CD spectroscopy were used to determine the fractional selectivity of the two fragments (and later domains) on a metal-by-metal basis. The high-resolution data allowed analysis of the fractional changes in binding site location selected as the metal binding domains formed. Our analysis is the first to show the stepwise preferences for both zinc and cadmium at physiologically relevant pH values. The data analysis provides detailed insight into the formation of the fully metalated protein and indicates that at pH 7.4 there is no significant trend to domain specificity for either zinc or cadmium. The ESI mass spectral data provide a quantitative domain selectivity index reflective of the K_F^{Cd}/K_F^{Zn} ratios for each of the seven metal exchange reactions.

METHODS

Purification of Recombinant Fragments. Preparation of isolated MT domain fragments followed previously reported methods.[44] The amino acid sequences for the isolated domains used in this study are based on the recombinant human MT1A sequence: the 38-residue β-MT domain fragment sequence (MGKAAAACSC ATGGSCTCTG SCKCKECKCN SCKKA-AAA) and the 41-residue α-MT domain fragment sequence (MGKAAAAC CSCCPMSCAK CAQGCVCKGA SEKCSCC-KKA AAA). Each of the corresponding DNA sequences was inserted as an N-terminal S-tag fusion protein into pET29a plasmids and individually expressed in *Escherichia coli* BL21-(DE3) with cadmium-supplemented growth medium. Each protein was expressed and purified separately as the cadmium-saturated form. All purified protein solutions were evacuated and saturated with argon to impede cysteine oxidation.

DOI: 10.1021/acs.biochem.5b00452
Biochemistry 2015, 54, 5006−5016

Preparation of Apo Fragments. Cadmium was removed from the purified, isolated MT domains. The protein solutions were acidified to pH 2.7 before the released cadmium was separated from the apoproteins on GE Sephadex G-25 size exclusion medium using formic acid in water (pH 2.7) as the eluent. The apoproteins were then concentrated and buffer exchanged with 5 mM ammonium formate (pH 7.4) using Millipore Amicon Ultra-4 centrifuge filter units (3 kDa MWCO). Protein concentrations of the final, pH-adjusted apoβMT and apoαMT solutions were determined by cadmium remetalation of small fractions of each protein monitored using UV−visible absorption (Cary 50, Varian Canada): ε_{250} values of 36000 and 45000 M^{-1} cm^{-1} for Cd_3-βMT and Cd_4-αMT, respectively.

Zinc and Cadmium Titrations. Stocks of 5 mM zinc acetate (Fisher Scientific) and 5 mM cadmium acetate (Acros Organics) were freshly prepared in deionized water, and the concentrations of zinc and cadmium were determined using atomic absorption spectroscopy (AA 240, Varian). **Caution:** *Cadmium acetate is a known carcinogen. Special care should be taken with its handling and disposal.* Equal concentrations of apoβMT and apoαMT were mixed in acid-washed vials, and the pH values of the resulting solutions were adjusted for the titration. Equivalents of zinc were then added under an argon atmosphere. Following each addition, the solution was equilibrated on ice for 3−5 min before the acquisition of ESI data. Longer equilibration times showed no significant change in the speciation of spectral data (data not shown). Once the fragments were both saturated with zinc, cadmium equivalents were added following a similar procedure. The room-temperature circular dichroism (CD) spectra of the solutions were also measured following each cadmium addition. Cadmium was added until the fragments had both exchanged all zinc and were cadmium-saturated. The titrations were each repeated in triplicate.

ESI-MS and CD Parametrizations. A Bruker Micro-TOF II instrument (Bruker Daltonics, Toronto, ON) operated in positive ion mode was used to collect the data. NaI was used as an external calibrant. The following settings were used: scan, m/z 500−3000; rolling average, 2; nebulizer, 2 bar; dry gas, 80 °C at a rate of 8.0 L/min; capillary, 4000 V; end plate offset, −500 V; capillary exit, 175 V; skimmer 1, 30.0 V; skimmer 2, 23.5 V; hexapole RF, 800 V. The spectra were collected for a minimum of 2 min and deconvoluted using the Maximum Entropy algorithm of the Bruker Compass DataAnalysis software package. A Jasco J810 spectropolarimeter was used to collect CD spectral data. The following scan parameters were used: step scan; range, 350−220 nm; data pitch, 1 nm; bandwidth, 0.5 nm; response, 1 s. Spectra were zeroed at 300 nm, and a three-point fast Fourier transform filter was applied to smooth the data.

RESULTS

The question we wish to answer concerns the binding location of the incoming metal during the isomorphous replacement of zinc by cadmium. To test which fragment the incoming metal occupies, we devised a series of competitive titrations in which the isolated α and β fragments of MT1A, used as a general model, could compete for incoming metals. Key to these competitive reactions is the fact that the two competing species are at equal concentrations. Subsequent metalation results in occupancy that will depend solely on the thermodynamically preferred distribution based on the relative magnitude of the formation constants. Thus, in all of the following experiments, the α and β fragments are always at equal concentrations and the metal occupancy will depend on the relative values of the seven formation constants ($K_{n,F}$, where n = 1−7) that govern the competitive reaction products.

Competitive Zinc Titration of MT Fragments: ESI-MS Data. In the process of initial metalation, the apoMT strand must rearrange the protein backbone to accommodate metal binding by the cysteine side chains. The relative abundancies in the ESI mass spectral data are representative of the relative concentrations of the species in solution, as demonstrated previously for zinc,[26] cadmium,[43] arsenic,[45] and bismuth[46] MTs. Figure 3 shows the mass spectral data for the competitive

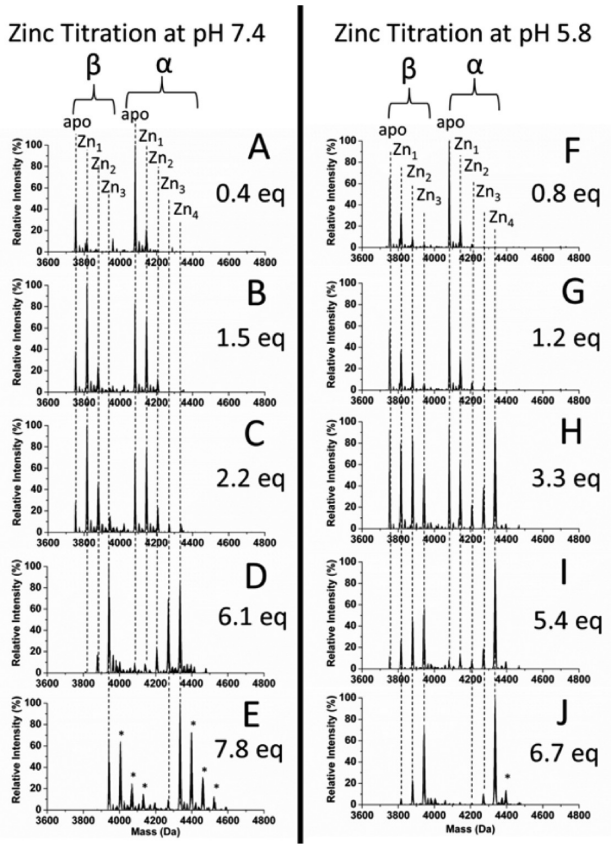

Figure 3. Representative deconvoluted ESI mass spectral data recorded during the competitive zinc titrations at pH 7.4 (A−E) and pH 5.8 (F−J) of equimolar mixtures of β-MT and α-MT. The important species are labeled with dashed lines. Asterisks indicate nonspecific zinc adducts.

zinc titrations of equimolar α and β at pH 7.4 and 5.8 as a function of added zinc. Though we have previously reported a similar titration,[47] those results were measured at pH 9.2, significantly beyond the physiological range. As this report demonstrates, such a large pH discrepancy can have effects on the metal binding properties, especially the metal distributions of Zn_n-MT, which differ quite significantly at all three pH values because of the pH dependence of the metal binding reactions.

As zinc is added stepwise to the competing domain fragments, we observe the sequential addition of zinc to both fragments shown in Scheme 2. As discussed above, because the binding sites are in direct competition for the zinc ions, the zinc is bound in a sequence that correlates with the order of the zinc affinities between the α and β domain fragments. For example,

DOI: 10.1021/acs.biochem.5b00452
Biochemistry 2015, 54, 5006−5016

at pH 7.4, Figure 3A–E shows that the β fragment binds a greater fraction of the first equivalent of zinc. In Figure 3B, where a total of 1.5 equiv of zinc has been added, the β distribution is dominated by Zn_1-βMT with some formation of Zn_2-βMT. The α species at the same point in the titration show the apo α form being more dominant than Zn_1-αMT. These data indicate that, under the conditions of the experiment, the first zinc binding event takes place in the β domain. At pH 5.8 (Figure 3F–J), the first zinc also binds to the β fragment. However, under these acidic conditions, the α fragment shows a higher degree of cooperativity compared to the binding at pH 7.4, and the order of subsequent zinc binding events is impacted. Though the α fragment begins to fill with zinc later in the titration, it saturates earlier than the β fragment. For example, in Figure 3I, where 5.4 equiv of zinc has been added, the α speciation is dominated by Zn_4-αMT, while the β fragment speciation shows significant apo-, Zn_1-, and Zn_2-βMT species. The competitive zinc titration data at pH 9.2 from ref 47 shows a degree of noncooperativity even higher than that shown here at pH 7.4, though the data sets do look similar.

Competitive Zinc Titration of MT Fragments: Speciation Profiles. To compare the titration data between the two domains as well as to observe differences within the fragments as a function of pH, we extracted the ESI speciation profiles for the two fragments as shown in Figure 4. This figure reveals information related to the overall binding properties of each of the two fragments. Panels A and B show the speciation of the α fragment and β fragment, respectively, as a function of added zinc. Zn_2-αMT and Zn_2-βMT are depressed relative to the other speciation traces. This indicates that the binding of the second and third zinc atoms in αMT facilitates the next binding events. We interpret this to imply that structural reorganization of the peptide backbone occurs such that the subsequent metalation to Zn_4-αMT is promoted. Figure 4C, which shows the zinc speciation of the α fragment as a function of added zinc at pH 5.8, highlights how this effect is even more pronounced at lower pH. At pH 5.8, the titration is dominated by the formation of the fully metalated Zn_4-αMT; the intermediate metalation states are all suppressed, and Zn_4-αMT appears earlier in the titration. This effect is not observed for the β fragment at pH 5.8 (Figure 4D), indicating that the zinc metalation mechanism of the α fragment is more sensitive to acidic conditions.

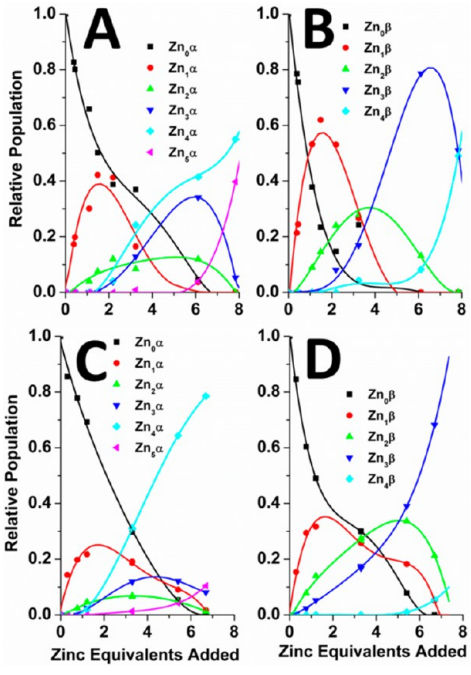

Figure 4. Extracted speciation profiles from the deconvoluted ESI mass spectral data. The panels show the relative populations of each species recorded during the competitive zinc titrations of equimolar mixtures of apo α (A and C) and apo β (B and D) MT at pH 7.4 (A and B) and pH 5.8 (C and D). Zinc was added stepwise to the solution of apo fragments until both fragments were zinc-saturated. The species have been plotted according to the stoichiometry of added zinc. One equivalent means the amount of zinc to fill one binding site. Lines have been added as guides linking the data points.

Competitive Cadmium Titrations of Zinc-Saturated Fragments at pH 7.4. Representative deconvoluted ESI mass spectral data for the competitive cadmium titration of zinc-saturated α-MT and β-MT fragments at pH 7.4 are shown in Figure 5. Figure 5, and the corresponding pH 5.8 titration data in Figure 7, reveals information about the location of cadmium exchange. Similar to how binding of zinc to the apo fragments depends on the zinc formation constants of the competitive reactions shown in Schemes 1 and 2, the site of the cadmium replacement depends on the relative magnitudes of the formation constants of the incoming cadmium and the

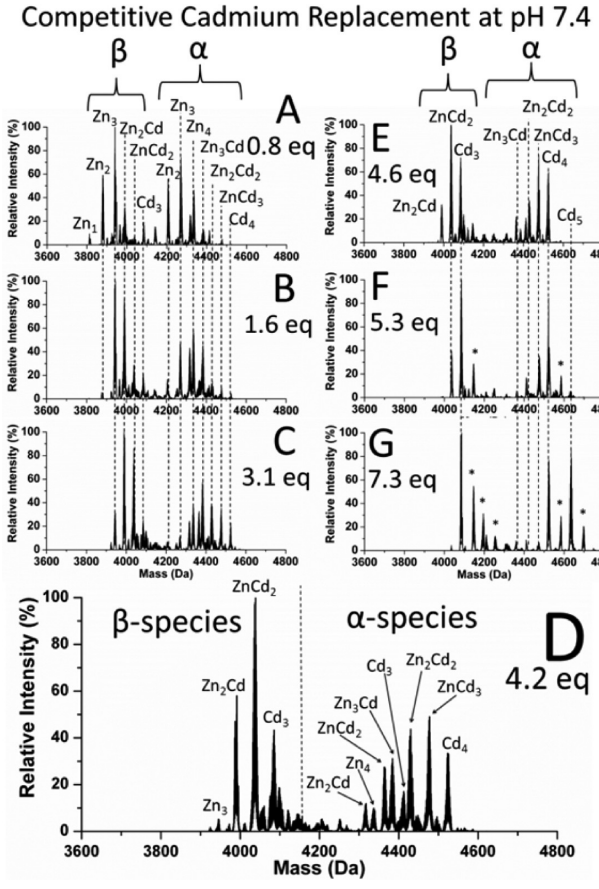

Figure 5. Representative ESI mass spectral data recorded during the competitive cadmium titration of an equimolar (31 μM) mixture of Zn_4-αMT and Zn_3-βMT at pH 7.4. The important species are labeled with dashed lines. Asterisks indicate nonspecific zinc adducts. Panel D shows expanded spectral data after 4.2 equiv has been added.

DOI: 10.1021/acs.biochem.5b00452
Biochemistry 2015, 54, 5006–5016

Scheme 1. Sequential Zinc Metalation Reactions of Apo$\beta\alpha$MT

$$apoMT + Zn^{2+} \overset{K_1}{\rightleftharpoons} Zn_1MT$$
$$Zn_1MT + Zn^{2+} \overset{K_2}{\rightleftharpoons} Zn_2MT$$
$$Zn_2MT + Zn^{2+} \overset{K_3}{\rightleftharpoons} Zn_3MT$$
$$\cdots$$
$$Zn_6MT + Zn^{2+} \overset{K_7}{\rightleftharpoons} Zn_7MT$$

Scheme 3. Sequential Cadmium Replacement Reactions of Zn_7-$\beta\alpha$MT

$$Zn_7MT + Cd^{2+} \overset{K_1}{\rightleftharpoons} Cd_1Zn_6MT + Zn^{2+}$$
$$Cd_1Zn_6MT + Cd^{2+} \overset{K_2}{\rightleftharpoons} Cd_2Zn_5MT + Zn^{2+}$$
$$Cd_2Zn_5MT + Cd^{2+} \overset{K_3}{\rightleftharpoons} Cd_3Zn_4MT + Zn^{2+}$$
$$\cdots$$
$$Cd_6ZnMT + Cd^{2+} \overset{K_7}{\rightleftharpoons} Cd_7MT + Zn^{2+}$$

outgoing zinc as shown in Schemes 3 and 4. This means that, starting with the first equivalent of added cadmium, the first zinc to exchange will depend on which site has the greatest K_F^{Cd}/K_F^{Zn} ratio. This will form the Zn_6Cd_1-MT species that is most thermodynamically preferred.

The ESI mass spectral data in Figure 5 show that, for the cadmium exchange at pH 7.4, cadmium binds to both domains simultaneously. At all steps in the cadmium titration, the speciation of the metals is mixed between the fragments. For example in Figure 5D, the expanded deconvoluted data for 4.2 equiv of added cadmium shows mixed metal β (Zn_3-, Zn_2Cd_1-, $ZnCd_2$-, and Cd_3-βMT) and mixed metal α (Zn_4-, Zn_3Cd_1-, Zn_2Cd_2-, $ZnCd_3$-, and Cd_4-αMT) metalation states.

The model scheme for the isomorphous replacement of zinc with cadmium (Scheme 3) follows a similar sequential mechanism as shown in Scheme 1. Each of the zinc atoms is replaced in sequence from zinc-saturated Zn_7-MT to cadmium-saturated Cd_7-MT in a series of seven, sequential, bimolecular reversible reactions. In this model, the populations of the various MT species are dependent on the K_F^{Cd}/K_F^{Zn} ratios for each of the metal exchange reactions.

The extracted speciation profiles for the pH 7.4 cadmium competitive exchange shown in Figure 5 are plotted in Figure 6. Panels A and B show the amounts of zinc bound to the α and β fragments, respectively, as a function of mole equivalents of added cadmium. These top two panels highlight the incremental decrease in zinc loading of the initially zinc-saturated fragments between the two domains (Zn_4-MT → Zn_3-MT → Zn_2-MT → Zn_1-MT → Zn_0-MT) as each zinc is substituted by the tighter binding cadmium ions. Panels C and D show the populations of increasing numbers of cadmium-bound species also as a function of added cadmium.

Competitive Cadmium Titrations of Zinc-Saturated Fragments at pH 5.8. Figure 7 shows deconvoluted mass spectral data for the zinc−cadmium competitive exchange reaction at pH 5.8. As cadmium is added, the zinc is replaced in a sequential manner within each fragment. Figure 7B shows how the first cadmium exchange reaction largely takes place in the β fragment.

The extracted ESI mass spectral data speciation profiles for the pH 5.8 competitive cadmium titration are shown in Figure 8. Again, we compare the different experimental speciation profiles based on relative populations, the population peak intensity, and population peak location to reveal information about the relative site occupancy following displacement of zinc with cadmium in the two fragments.

Circular Dichroism. The CD spectra that were simultaneously measured for each cadmium addition during the stepwise cadmium titrations are shown in Figure 9. At pH 7.4 (Figure 9A), there is an initial increase in the dichroism at 250 nm as the cadmium displaces a single zinc. A red shift to a 260 nm shoulder is indicative of the clustering to nominally cadmium-saturated Cd_3-βMT and Cd_4-αMT. Finally, the intensity maximum shifts back to 250 nm because of the formation of Cd_5-αMT at the end of the titration, as has been previously described.[48] The pH 5.8 data (Figure 9B) have similar spectral features. The key difference between the spectral profiles is the absence of the strongly isodichroic point at 250 nm in the pH 7.4 spectra. This is likely due to the fact that under acidic conditions, the formation of Cd_4-αMT clusters is preferred, meaning that the α fragment exchanges earlier in the titration at lower pH values.

DISCUSSION

Extracting Metal Binding Properties of MT Using Competitive Titrations. There has been considerable discussion regarding the metal binding constants associated with each metal that binds to MT.[17,25,26,40,49−53] Initial reports of binding of zinc to MT had suggested that all seven zinc ions were bound with approximately the same binding constant.[40] This model was refined by Maret and co-workers[25] when they determined four independent binding constants (where the four highest-affinity sites bound zinc with approximately the same K_F and the three remaining sites had sequentially decreasing affinities) and again by our group when we reported

Scheme 2. Competitive and Sequential Metalation Reactions of ApoβMT and ApoαMT

$$apo\beta MT + Zn^{2+} \overset{K_{1\beta}}{\rightleftharpoons} Zn_1\beta MT$$
$$Zn_1\beta MT + Zn^{2+} \overset{K_{2\beta}}{\rightleftharpoons} Zn_2\beta MT$$
$$Zn_2\beta MT + Zn^{2+} \overset{K_{3\beta}}{\rightleftharpoons} Zn_3\beta MT$$

$$apo\alpha MT + Zn^{2+} \overset{K_{1\alpha}}{\rightleftharpoons} Zn_1\alpha MT$$
$$Zn_1\alpha MT + Zn^{2+} \overset{K_{2\alpha}}{\rightleftharpoons} Zn_2\alpha MT$$
$$Zn_2\alpha MT + Zn^{2+} \overset{K_{3\alpha}}{\rightleftharpoons} Zn_3\alpha MT$$
$$Zn_3\alpha MT + Zn^{2+} \overset{K_{4\alpha}}{\rightleftharpoons} Zn_4\alpha MT$$

DOI: 10.1021/acs.biochem.5b00452
Biochemistry 2015, 54, 5006−5016

Scheme 4. Competitive and Sequential Cadmium Replacement Reactions of Zn_4-αMT and Zn_3-βMT

$$Zn_3\beta MT + Cd^{2+} \underset{}{\overset{K_{1\beta}}{\rightleftharpoons}} Cd_1Zn_2\beta MT + Zn^{2+} \qquad Zn_4\alpha MT + Cd^{2+} \underset{}{\overset{K_{1\alpha}}{\rightleftharpoons}} Cd_1Zn_3\alpha MT + Zn^{2+}$$

$$Cd_1Zn_2\beta MT + Cd^{2+} \underset{}{\overset{K_{2\beta}}{\rightleftharpoons}} Cd_2Zn_1\beta MT + Zn^{2+} \qquad Cd_1Zn_3\alpha MT + Cd^{2+} \underset{}{\overset{K_{2\alpha}}{\rightleftharpoons}} Cd_2Zn_2\alpha MT + Zn^{2+}$$

$$Cd_2Zn_1\beta MT + Cd^{2+} \underset{}{\overset{K_{3\beta}}{\rightleftharpoons}} Cd_3\beta MT + Zn^{2+} \qquad Cd_2Zn_2\alpha MT + Cd^{2+} \underset{}{\overset{K_{3\alpha}}{\rightleftharpoons}} Cd_3Zn_1\alpha MT + Zn^{2+}$$

$$Cd_3Zn_1\alpha MT + Cd^{2+} \underset{}{\overset{K_{4\alpha}}{\rightleftharpoons}} Cd_4\alpha MT + Zn^{2+}$$

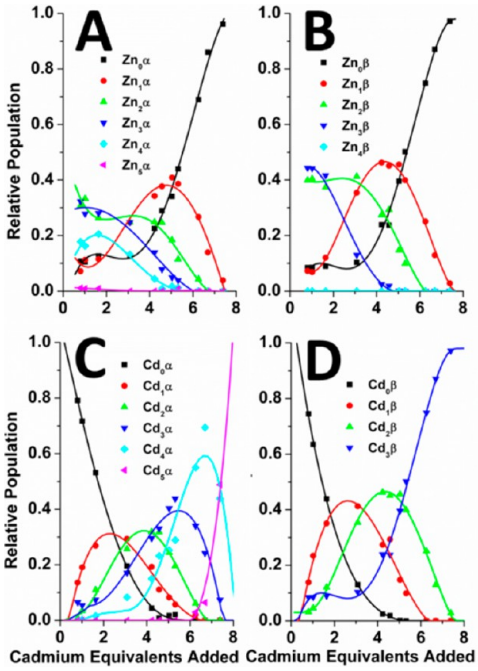

Figure 6. Extracted speciation profiles from the deconvoluted ESI mass spectral data. The panels show the relative populations of each species recorded during competitive titrations of an equimolar (31 μM) mixture of Zn_4-αMT (A and C) and Zn_3-βMT (B and D) with cadmium at pH 7.4. The species populations have been plotted according to the stoichiometry of bound zinc (A and B) and cadmium (C and D). Lines have been added as guides linking the data points.

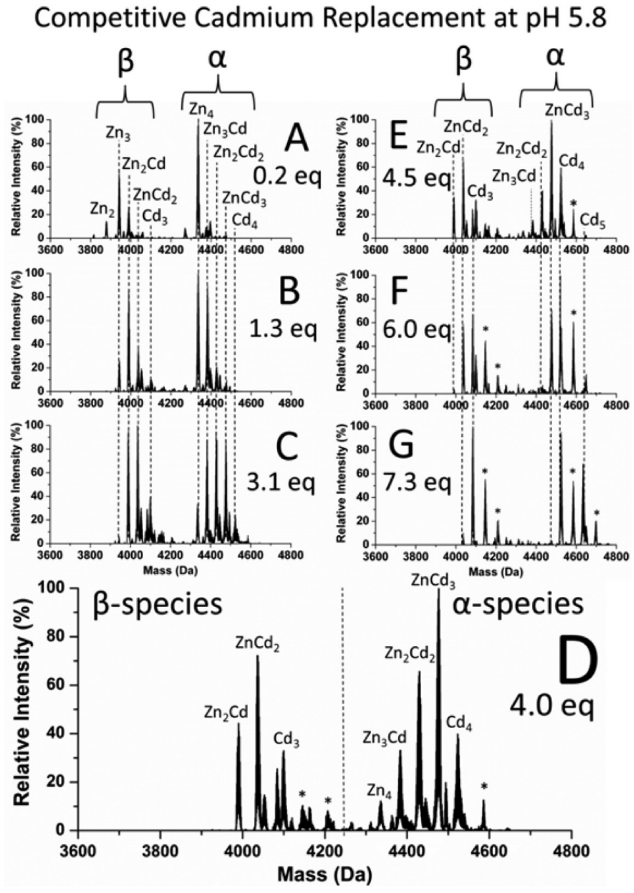

Figure 7. ESI mass spectral data recorded during the competitive cadmium titration of an equimolar (34 μM) mixture of Zn_4-αMT and Zn_3-βMT at pH 5.8. The important species are labeled with dashed lines. Panel D shows expanded spectral data after 4.0 equiv of Cd^{2+} has been added.

the values of all seven independent zinc binding constants, one for each of the zinc binding events.[26] As previous results have demonstrated, MTs bind zinc and cadmium with high affinities.[39] The fluxional nature of the apoMT strand, the metal-dependent folding that occurs during metalation, and the mobility of the metals between and within the protein all require careful and innovative experimental designs to assign independent affinity constants.

Competitive titrations have previously been used to study the metalation processes of MTs.[26,28,47,49] In the formation of metal-saturated final products, the MTs pass through partially metalated intermediates. For example, the formation of Zn_4-MT follows Zn_3-MT as an intermediate, which requires formation of Zn_2-MT, and so on back to apoMT (Scheme 1). Similar schemes have been proposed for the zinc,[26] cadmium,[43] and arsenic[45] metalation mechanisms for MT.[50] Some of the proposed functions of MT are accessible only when the protein is not metal-saturated. For example, the homeostatic control of zinc requires both acquisition and donation of zinc,[54] necessitating the presence of unsaturated MTs *in vivo*; studies have shown the presence of these unsaturated MTs *in vivo*.[55] Differences in the zinc transfer potentials of the two domains have also been discussed in relation to the importance of the domain structure of the intact MT protein.[53]

It is important to note that we are extrapolating information about the intact protein (Scheme 1) on the basis of results from titrations of the separated domains (Scheme 2). Previous work has suggested that the two isolated domains possess properties that differ from those of the intact peptide.[53] Determining the metal distribution in the whole protein, however, is complicated by the lability of the metals, especially following chromatographic separations and/or chemical modifications common in other studies of domain specificity. Though the affinity constants of the separated domains are changed upon domain separation (because of increased fluxionality and options for domain reorganization in the larger intact protein strand), we expect that the properties governing metal distribution between

DOI: 10.1021/acs.biochem.5b00452
Biochemistry 2015, 54, 5006−5016

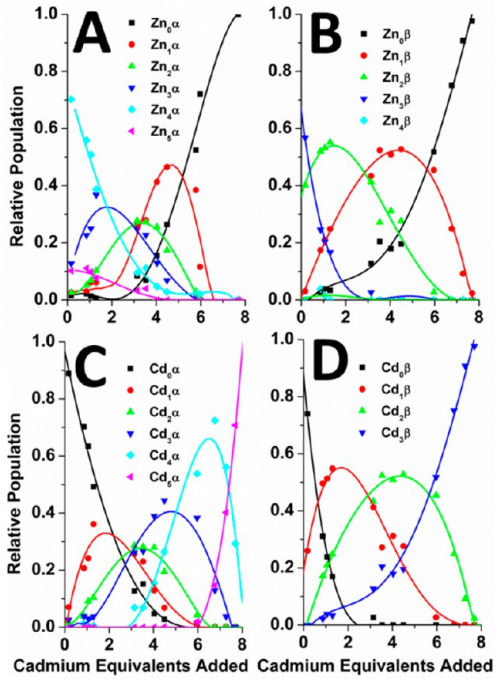

Figure 8. Extracted speciation profiles, from the deconvoluted ESI mass spectral data. The data in the panels were recorded during the competitive cadmium titrations of an equimolar (34 μM) mixture of Zn-αMT (A and C) and Zn-βMT (B and D) at pH 5.8. The species have been plotted according to the stoichiometry of bound zinc (A and B) and cadmium (C and D). Lines have been added as guides linking the data points.

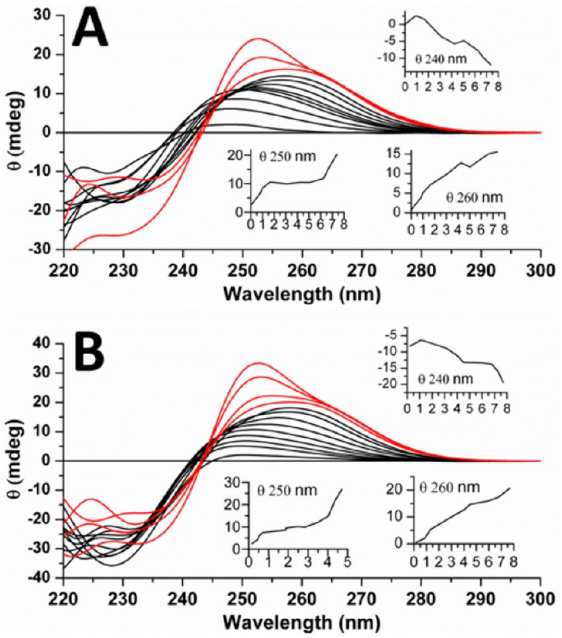

Figure 9. CD spectroscopic data measured for the competitive cadmium titration starting from an equimolar (31 and 34 μM) mixture of Zn_4-αMT and Zn_3-βMT at (A) pH 7.4 and (B) 5.8. The inset boxes show the change in ellipticity at 240, 250, and 260 nm as a function of equivalents of Cd^{2+} added. Red lines indicate solutions containing Cd_5-αMT based on ESI mass spectral data.

the domains remain essentially unchanged, as has been demonstrated for metal-saturated MTs.[56] Assuming that the metalation reactions follow a purely domain specific mechanism, it is likely that the separated domains would enhance this feature because the number of interdomain interactions that would result in property differences between the separated domains and intact protein is reduced.[53] We will return to discuss evidence of interdomain interactions below. Arsenic binding studies showed that the trend in binding was maintained in the isolated domains relative to that of the intact protein.[45,57]

At the MT protein concentrations used in this study, dimerization of the MT species, either in solution or in the ESI ionization process, is possible. However, we saw no evidence of dimer formation in the resulting ESI mass spectral data. We also note that at higher metal concentrations, such as the end of the cadmium titration of mixed Zn-MTs (where total $[Cd^{2+}]$ + $[Zn^{2+}] \approx 500$ μM), nonspecific metal binding may occur during the electrospray process that does not directly correspond to the solution phase metalation states. There were some nonspecific adducts formed toward the end of the zinc titration experiments, especially at higher pH (Figure 3E). Because of the fact that the cadmium added replaced the zinc bound stoichiometrically, we are confident that this effect was minimal for the conditions of the cadmium experiments.

Comparison of pH 7.4 and pH 5.8 Data. Via substitution of zinc with cadmium in one MT species, the vertical panels in Figures 6 and 8 (zinc loss vs cadmium bound) should result in mirror images. Each cadmium binding event must correspond to a zinc loss. However, we see interesting speciation profiles for these competition reactions because both domain fragments are competing for the added cadmium and released zinc. For each metal substitution step, the concentration of free zinc in the solution changes, and 7 equiv of free zinc is released by the end of the titration. As shown in Scheme 4, the increases in free zinc concentration compete with cadmium binding, which leads to a redistribution of the zinc and cadmium among the two fragments governed by the thermodynamic minimum of the K_F^{Cd}/K_F^{Zn} ratio.

Seven Cadmium for Seven Zincs. One of the most discussed functions of MT is its ability to detoxify heavy metals. This occurs *in vivo* through the replacement of the zinc in Zn-MT with cadmium. *In vivo*, MTs predominantly exist as the zinc-bound form (Zn_n-MT, where n = 4–7) and not the apo form, and the binding of cadmium to MT is a result of the metal exchange. In this study, we used Zn-MT1A fragments as the starting point of the cadmium exchange competition, which may account for discrepancies between this work and previously published results that showed that the cadmium binding was cooperative and α-domain selective for experiments that used MT2A.[53] Cadmium binds with an affinity (K_F) higher than that of zinc; zinc binding and cadmium binding have long been considered isomorphous.

Past work has suggested that this exchange may occur in a domain specific manner, where the first four added cadmiums are primarily localized to the α domain of the full MT. This mechanism was largely developed from data obtained through spectroscopic techniques such as UV–visible absorption, CD, MCD, NMR, and EPR and on the assumption that the MT metalation state was largely homogeneous. Except for NMR (whose signal intensity is resolved for only the metal-saturated and nonfluxtional clusters and at millimolar concentrations), these techniques all provide the average metal load of all the concurrent species that exist. However, as shown by numerous ESI-MS studies, the metalation speciation of the MT strand is

DOI: 10.1021/acs.biochem.5b00452
Biochemistry 2015, 54, 5006–5016

significantly heterogeneous, with a spread of speciation summing to the average metal loads. Our data unambiguously confirm and support this distributed heterogeneous binding mode (Figures 3, 5, and 7).

Modeling Site Selection Mechanisms between the α and β Domains. Three models of metal selectivity between the domains (or, in the case of our competition experiments, the domain fragments) are shown in Figure 10. These models show the expected experimental results for a completely α (panel A) or β (panel B) selective mechanism, as well as for a mechanism in which there is no selectivity between the fragments (panel C). Figure 10 provides the average metal loading (top panels) and domain selectivity (bottom panels) of those three models. The relative selectivity is defined as the difference in stepwise occupancy between the domains for each incoming metal. A value of +1 says the incoming metal bound specifically in the α domain, and a value of −1 says the incoming metal bound specifically in the β domain. A value of zero says the incoming metal was distributed evenly between both randomly, meaning no domain specificity.

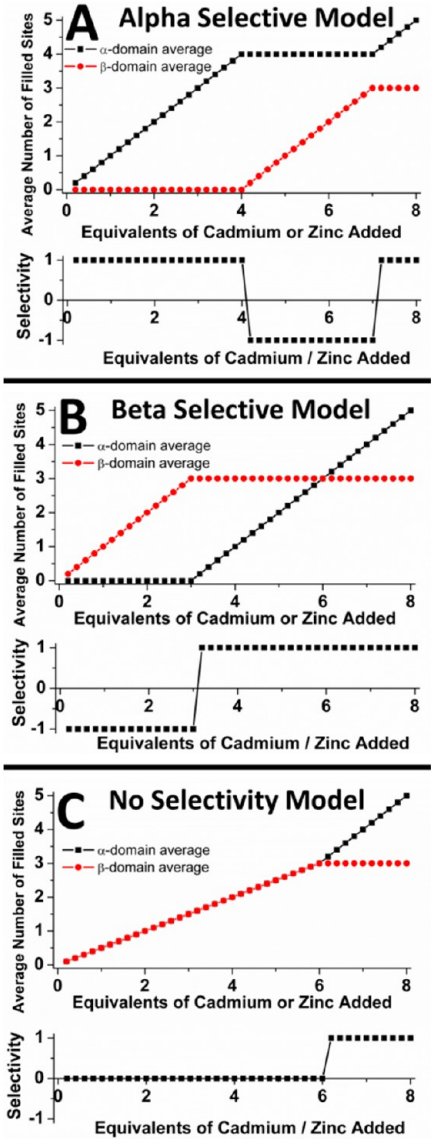

Figure 10. Models of selectivity in binding of zinc and cadmium to MT. Shown are three possible mechanisms for binding of metal to MTs: (A) an α selective model, (B) a β selective model, and (C) a model in which there is no specific selectivity and, therefore, completely random binding between the domains. Top panels show the approximate speciation for the average metal loading in the α and β domains. Bottom panels show the domain selectivity during the course of the titration (+1 for α domain binding, −1 for β domain binding).

The first model shows the domain occupancy with α selectivity where the first 4 equiv of added metal binds to only the α domain (Figure 10A). Once the α domain is filled with 4 equiv, the next 3 equiv fills the β domain. The final equivalent supermetalates the α domain to form $(Cd/Zn)_5$-αMT as has been previously described.[48] The modeled selectivity for the α domain over the β domain is based on the order of the binding constants that describe the reactions in the competition experiments (Schemes 2 and 4 and discussed above). In this model, the four sites with the highest affinities are located exclusively in the α domain.

The second model shows the effect on occupancy with β selectivity; the first 3 equiv of added metal binds to only the β domain (Figure 10B). Once the β domain is filled, the α domain binds the remaining incoming metals. Again, the modeled selectivity for the β domain over the α domain is due to the order of the binding constants that would generate this β selective model. In this model, the binding constants in the β domain have affinities higher than that of the α domain, and the binding is β-directed.

In the final model, there is no specific selectivity between the domains, and it is clear that the first 6 equiv of added metal binds equally to both domains (Figure 10C). After the first 6 equiv has been added, the β domain is filled and the α domain binds the final equivalent to complete the titration. Once again, this model is based on the relative magnitudes of the binding constants at each point during the metal titrations. For this model, the first six binding constants are mixed between the two domains and neither domain shows selectivity.

Comparison of the Experimental Data and the Models. Figure 11 shows the stepwise, metal-by-metal selectivity, calculated from the ESI-MS data described above, as zinc was added to the mixed α and β fragments at (A) pH 7.4 and (B) 5.8. The dashed lines indicate the occupancy per addition if there was 100% selectivity for either the α fragment (+1) or the β fragment (−1). It is clear that, at pH 7.4, the more numerous cysteines in the α fragment bias the results such that there is a trend toward the α fragment. The conclusion is that there is no specific selectivity that cannot be ascribed to the greater numbers of cysteines in the α fragment (11 vs 9). At pH 5.8, however, there is evidence of weak α domain selectivity. Again, after the first zinc binds to the β fragment, the zinc ions bind to the α fragment until the α cluster is filled and the remaining zinc ions fill the β fragment. Our conclusion is that under acidic conditions, there is a weak selectivity. The α fragment binds a greater fraction of, but not all of, the added zinc.

We next turn to data recorded for the stepwise displacement of zinc by cadmium (Figure 12). This reaction has long been studied because of the toxicological implications of cadmium exposure, and the initial structural data came from cadmium-containing protein. In the experiments analyzed here, we are able to identify the fragment (and later the domain) selection that is the precursor to the domain specificity mentioned in the literature. The ESI-MS data provide far more detail than other techniques. Figure 12 provides the analysis of the mass spectral

DOI: 10.1021/acs.biochem.5b00452
Biochemistry 2015, 54, 5006−5016

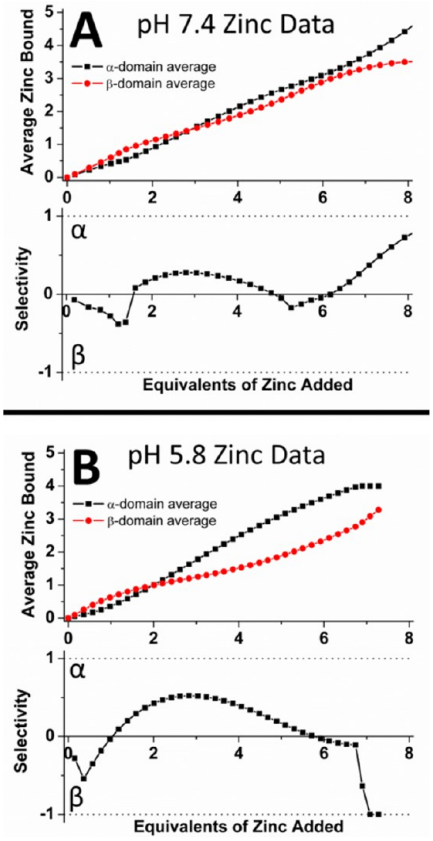

Figure 11. Experimental data for the zinc titrations at (A) pH 7.4 and (B) 5.8. Top panels show the calculated average zinc loading by each fragment over the stepwise titration shown in Figures 3 and 4. Bottom panels show the differential domain selectivity of each zinc addition (+1 for α domain binding, −1 for β domain binding).

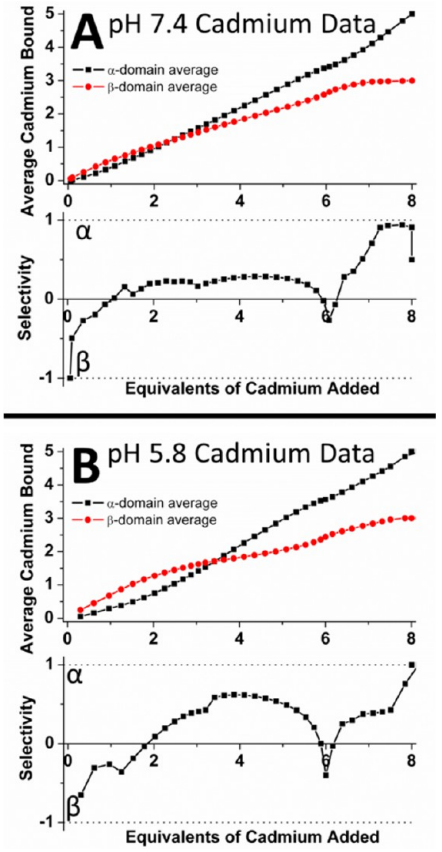

Figure 12. Experimental data for the cadmium titrations at (A) pH 7.4 and (B) 5.8. Top panels show the calculated average cadmium loading by each fragment over the stepwise titration shown in Figures 5−8. Bottom panels show the differential domain selectivity of each cadmium addition (+1 for α domain binding, −1 for β domain binding).

data to assess the fragment selection for each addition of cadmium. We note that for each cadmium added, a zinc is displaced, increasing $[Zn]_{free}$. At pH 7.4 (Figure 12A), we see that the two domains fill with cadmium evenly.

The selectivity shows a pattern almost exactly the same as that for zinc. That is, the first cadmium displaces a zinc in the β cluster (we now talk about clusters because the two fragments are saturated with zinc so they exist as the two clustered species, Zn_4Cys_{11}-α-MT and Zn_3Cys_9-β-MT). There is, however, little evidence of more than minor selectivity for the α domain at pH 7.4. We conclude that, at pH 7.4, there is little domain specificity for cadmium displacing zinc.

At pH 5.8 (Figure 12B), there is clearly an increase in the frequency of selection of the α domain. The first cadmium still displaces the zinc in the β cluster, but then the α domain is preferred. Comparison with the theoretical simulations shows that the preference is nowhere near domain specific; rather, there is again a preference for the α domain.

Potential for Interdomain Interactions and Comparison to Existing Data. It is possible that the separated domains possess metal binding properties, including domain specificity, different from those in the intact protein, because the chain lengths and cysteine content are different. For example, we have previously described a model metalation pathway for the intact protein, based on the results of metal titrations to MTs at basic pH, where the first five metals added to apoMT bind in a beaded fashion, forming $(M^{II})Cys_4$ beads before clustering, following the addition of two additional metals to the two-domain protein.[47] By definition, this model meant that the metals bound initially in a non-domain specific fashion because, for example, the $(M^{II})_4(Cys)_{16}$-MT species uses 16 of the total 20 cysteines in the binding of the metals, more than occur in either domain. Because the domain structure is not formed at this point, we cannot determine if the metals bound in the early stages of the titration, $(M^{II})_{1-3}$-MTs, occurred in either the N-terminal or C-terminal region of the protein first. The data presented in this report of the separated domain fragments of MT1A extend the data in support of the model [at least for $(M^{II})_{1-2}$-MTs], showing that the metals are distributed between the fragments at all points in the titration. The results also hint at interactions between the domains in the intact MTs that may facilitate metal binding and change the metal binding properties.

These results contrast with those of other studies of domain selectivity described above,[32,34,35,60] from most notably NMR experiments of metal titrations of MTs. However, data recently reported by Chen et al. showed, using NEM modification of intact MT2 studied by ESI-MS/MS, that the stable Cd_4-MT species had the cadmium bound exclusively to the α domain at pH 7.4.[58] An even more recent study by the same group suggested that other intermediate metalation states had cadmium bound to both domains and suggested that the Cd_4-MT was due to metal rearrangements to form a thermodynamically stable product.[24]

DOI: 10.1021/acs.biochem.5b00452
Biochemistry 2015, 54, 5006−5016

This apparent discrepancy in the determination of the presence of domain selectivity may be due to methodological differences in the studies; for example, NEM (and other) modifications may influence the cadmium binding and "push" the cadmium toward α-domain selectivity, which could possibly arise from NEM reaction rate differences between the domains. Alternatively, connection of the domains in the intact protein may permit the reorganization of the bound metals from sites distant on the sequence that is more difficult for the separated domains to achieve. MT−MT metal transfers through direct protein−protein interactions have been reported for arsenic transfer between MT species,[59] which is significantly less labile than zinc or cadmium. Finally, the difference in the experimental data could simply be due to the different isoforms having different binding affinities for cadmium, as it has been suggested that different MTs do show different metal selectivities.[60] Clearly, a careful and direct comparison between the metal binding properties of MT1 and MT2, studied under the same conditions, using the same methodology is required.

CONCLUSIONS

It is becoming increasingly apparent that the traditional model of the two-domain structure of MTs is an insufficient descriptor of the functionality of MT species. It is also clear from many other experiments that the metals in MTs are labile and occupy those sites with the largest binding constants. Here, we have investigated the role of the two isolated domain fragments of MT1A in zinc acquisition and cadmium exchange using competitive metal titrations at two biologically relevant pHs. The data showed subtle cadmium bias for the α fragment at lower pH. All species showed mixed metalation states at all points in the competitive cadmium exchange titration, for both the α and β fragments.

The experimental data, supported by the models, unambiguously show that, under these conditions, neither zinc nor cadmium follows a domain selective binding mechanism between either of the isolated domains. The binding affinity constants clearly span both fragments in their magnitude, resulting in a distribution of metals. This distribution is driven by the interplay of these binding affinities (K_F^{Cd}/K_F^{Zn}) that are close in magnitude, resulting in the nonspecific site selection between the fragments.

AUTHOR INFORMATION

Corresponding Author

*E-mail: martin.stillman@uwo.ca. Phone: (519) 661-3821. Fax: (519) 661-3022.

Funding

We acknowledge financial support from the Natural Sciences and Engineering Research Council of Canada for Discovery and RTI grants (to M.J.S.) as well as graduate scholarships (to T.B.J.P. and G.W.I.).

Notes

The authors declare no competing financial interest.

ACKNOWLEDGMENTS

We thank Ms. Tiffany Jeen [Inorganic Chemistry Exchange from the University of Saskatchewan (Saskatoon, SK) supported by a NSERC-USRA scholarship at the University of Western Ontario] for preliminary work.

ABBREVIATIONS

MT, mammalian metallothionein; MT1A, human metallothionein 1A isoform; ESI-MS, electrospray ionization mass spectrometry; MWCO, molecular weight cutoff; CD, circular dichroism; apoMT, metal-free metallothionein; MCD, magnetic circular dichroism; EPR, electron paramagnetic resonance; $[Zn]_{free}$, concentration of free zinc in solution.

REFERENCES

(1) Berg, J. M., and Shi, Y. (1996) The galvanization of biology: A growing appreciation for the roles of zinc. *Science 271*, 1081−1085.
(2) Capdevila, M., and Atrian, S. (2011) Metallothionein protein evolution: A miniassay. *JBIC, J. Biol. Inorg. Chem. 16*, 977−989.
(3) Blindauer, C. A. (2015) Advances in the molecular understanding of biological zinc transport. *Chem. Commun. 51*, 4544−4563.
(4) Waisberg, M., Joseph, P., Hale, B., and Beyersmann, D. (2003) Molecular and cellular mechanisms of cadmium carcinogenesis. *Toxicology 192*, 95−117.
(5) Shimoda, R., Nagamine, T., Takagi, H., Mori, M., and Waalkes, M. P. (2001) Induction of apoptosis in cells by cadmium: Quantitative negative correlation between basal or induced metallothionein concentration and apoptotic rate. *Toxicol. Sci. 64*, 208−215.
(6) Waalkes, M. P. (2000) Cadmium carcinogenesis in review. *J. Inorg. Biochem. 79*, 241−244.
(7) Bertin, G., and Averbeck, D. (2006) Cadmium: Cellular effects, modifications of biomolecules, modulation of DNA repair and genotoxic consequences (a review). *Biochimie 88*, 1549−1559.
(8) Outten, C. E., and O'Halloran, T. V. (2001) Femtomolar sensitivity of metalloregulatory proteins controlling zinc homeostasis. *Science 292*, 2488−2492.
(9) Waisberg, M., Joseph, P., Hale, B., and Beyersmann, D. (2003) Molecular and cellular mechanisms of cadmium carcinogenesis. *Toxicology 192*, 95−117.
(10) Coyle, P., Philcox, J., Carey, L., and Rofe, A. (2002) Metallothionein: The multipurpose protein. *Cell. Mol. Life Sci. 59*, 627−647.
(11) Stillman, M., Cai, W., and Zelazowski, A. (1987) Cadmium binding to metallothioneins. Domain specificity in reactions of alpha and beta fragments, apometallothionein, and zinc metallothionein with Cd^{2+}. *J. Biol. Chem. 262*, 4538−4548.
(12) Margoshes, M., and Vallee, B. L. (1957) A cadmium binding protein from equine kindney cortex. *J. Am. Chem. Soc. 79*, 4813−4814.
(13) Capdevila, M., Bofill, R., Palacios, Ò., and Atrian, S. (2012) State-of-the-art of metallothioneins at the beginning of the 21st century. *Coord. Chem. Rev. 256*, 46−62.
(14) Klaassen, C. D., Liu, J., and Choudhuri, S. (1999) Metallothionein: An intracellular protein to protect against cadmium toxicity. *Annu. Rev. Pharmacol. Toxicol. 39*, 267−294.
(15) Palmiter, R. D. (2004) Protection against zinc toxicity by metallothionein and zinc transporter 1. *Proc. Natl. Acad. Sci. U. S. A. 101*, 4918−4923.
(16) Kang, Y. J. (2006) Metallothionein redox cycle and function. *Exp. Biol. Med. 231*, 1459−1467.
(17) Maret, W., and Vallee, B. L. (1998) Thiolate ligands in metallothionein confer redox activity on zinc clusters. *Proc. Natl. Acad. Sci. U. S. A. 95*, 3478−3482.
(18) Thirumoorthy, N., Shyam Sunder, A., Manisenthil Kumar, K., Senthil kumar, M., Ganesh, G., and Chatterjee, M. (2011) A Review of Metallothionein Isoforms and their Role in Pathophysiology. *World J. Surg. Oncol. 9*, 54.
(19) Robbins, A. H., McRee, D. E., Williamson, M., Collett, S. A., Xuong, N. H., Furey, W. F., Wang, B. C., and Stout, C. D. (1991) Refined crystal structure of Cd, Zn metallothionein at 2.0 Å resolution. *J. Mol. Biol. 221*, 1269−1293.
(20) Sutherland, D. E. K., and Stillman, M. J. (2014) Challenging conventional wisdom: Single domain metallothioneins. *Metallomics 6*, 702−728.

DOI: 10.1021/acs.biochem.5b00452
Biochemistry 2015, 54, 5006−5016

(21) Nielson, K. B., Atkin, C. L., and Winge, D. R. (1985) Distinct metal-binding configurations in metallothionein. *J. Biol. Chem. 260*, 5342−5350.
(22) Sutherland, D. E. K., and Stillman, M. J. (2011) The "magic numbers" of metallothionein. *Metallomics 3*, 444−463.
(23) Furey, W., Robbins, A., Clancy, L., Winge, D., Wang, B., and Stout, C. (1986) Crystal structure of Cd,Zn metallothionein. *Science 231*, 704−710.
(24) Chen, S.-H., Chen, L., and Russell, D. H. (2014) Metal-induced conformational changes of human metallothionein-2A: A combined theoretical and experimental study of metal-free and partially metalated intermediates. *J. Am. Chem. Soc. 136*, 9499−9508.
(25) Krężel, A., and Maret, W. (2007) Dual nanomolar and picomolar Zn(II) binding properties of metallothionein. *J. Am. Chem. Soc. 129*, 10911−10921.
(26) Pinter, T. B. J., and Stillman, M. J. (2014) The zinc balance: Competitive zinc metalation of carbonic anhydrase and metallothionein 1A. *Biochemistry 53*, 6276−6285.
(27) Stillman, M. J., and Zelazowski, A. (1988) Domain specificity in metal binding to metallothionein. A circular dichroism and magnetic circular dichroism study of cadmium and zinc binding at temperature extremes. *J. Biol. Chem. 263*, 6128−6133.
(28) Połeć Pawlak, K., Palacios, Ò., Capdevila, M., González-Duarte, P., and Łobiński, R. (2002) Monitoring of the metal displacement from the recombinant mouse liver metallothionein Zn7-complex by capillary zone electrophoresis with electrospray MS detection. *Talanta 57*, 1011−1017.
(29) Stillman, M. J., and Zelazowski, A. J. (1989) Domain-specificity of Cd^{2+} and Zn^{2+} binding to rabbit liver metallothionein 2. Metal ion mobility in the formation of Cd_4-metallothionein alpha-fragment. *Biochem. J. 262*, 181−188.
(30) Boulanger, Y., Armitage, I. M., Miklossy, K. A., and Winge, D. R. (1982) ^{113}Cd NMR study of a metallothionein fragment. Evidence for a two-domain structure. *J. Biol. Chem. 257*, 13717−13719.
(31) Boulanger, Y., Goodman, C. M., Forte, C. P., Fesik, S. W., and Armitage, I. M. (1983) Model for mammalian metallothionein structure. *Proc. Natl. Acad. Sci. U. S. A. 80*, 1501−1505.
(32) Otvos, J. D., and Armitage, I. M. (1980) Structure of the metal clusters in rabbit liver metallothionein. *Proc. Natl. Acad. Sci. U. S. A. 77*, 7094−7098.
(33) Good, M., Hollenstein, R., Sadler, P. J., and Vasak, M. (1988) Cadmium-113 NMR studies on metal-thiolate cluster formation in rabbit cadmium(II) metallothionein: evidence for a pH dependence. *Biochemistry 27*, 7163−7166.
(34) Vazquez, F., and Vasak, M. (1988) Comparative ^{113}Cd-NMR studies on rabbit $^{113}Cd_7$-,(Zn_1, Cd_6)-and partially metal-depleted $^{113}Cd_6$-metallothionein-2a. *Biochem. J. 253*, 611−614.
(35) Otvos, J. D., Engeseth, H. R., and Wehrli, S. (1985) Preparation and cadmium-113 NMR studies of homogeneous reconstituted metallothionein: reaffirmation of the two-cluster arrangement of metals. *Biochemistry 24*, 6735−6740.
(36) Nettesheim, D. G., Engeseth, H. R., and Otvos, J. D. (1985) Products of metal exchange reactions of metallothionein. *Biochemistry 24*, 6744−6751.
(37) Messerle, B. A., Schäffer, A., Vašák, M., Kägi, J. H. R., and Wüthrich, K. (1990) Three-dimensional structure of human [$^{113}Cd_7$]-metallothionein-2 in solution determined by nuclear magnetic resonance spectroscopy. *J. Mol. Biol. 214*, 765−779.
(38) Robbins, A., McRee, D., Williamson, M., Collett, S., Xuong, N., Furey, W., Wang, B., and Stout, C. (1991) Refined crystal structure of Cd, Zn metallothionein at 2.0 Åresolution. *J. Mol. Biol. 221*, 1269−1293.
(39) Byrd, J., and Winge, D. R. (1986) Cooperative cluster formation in metallothionein. *Arch. Biochem. Biophys. 250*, 233−237.
(40) Petering, D. H., and Fowler, B. A. (1986) Roles of metallothionein and related proteins in metal metabolism and toxicity: problems and perspectives. *Environ. Health Perspect. 65*, 217−224.
(41) Vašák, M. (1991) Metal removal and substitution in vertebrate and invertebrate metallothioneins. In *Methods in Enzymology* (James, F., and Riordan, B. L. V., Eds.) pp 452−458, Academic Press, San Diego.
(42) Nielson, K. B., and Winge, D. R. (1983) Order of metal binding in metallothionein. *J. Biol. Chem. 258*, 13063−13069.
(43) Sutherland, D. E. K., and Stillman, M. J. (2008) Noncooperative cadmium(II) binding to human metallothionein 1a. *Biochem. Biophys. Res. Commun. 372*, 840−844.
(44) Merrifield, M. E., Huang, Z., Kille, P., and Stillman, M. J. (2002) Copper speciation in the α and β domains of recombinant human metallothionein by electrospray ionization mass spectrometry. *J. Inorg. Biochem. 88*, 153−172.
(45) Ngu, T. T., Easton, A., and Stillman, M. J. (2008) Kinetic analysis of arsenic-metalation of human metallothionein: Significance of the two-domain structure. *J. Am. Chem. Soc. 130*, 17016−17028.
(46) Ngu, T. T., Krecisz, S., and Stillman, M. J. (2010) Bismuth binding studies to the human metallothionein using electrospray mass spectrometry. *Biochem. Biophys. Res. Commun. 396*, 206−212.
(47) Summers, K. L., Sutherland, D. E. K., and Stillman, M. J. (2013) Single-domain metallothioneins: Evidence of the onset of clustered metal binding domains in Zn-rhMT 1a. *Biochemistry 52*, 2461−2471.
(48) Rigby Duncan, K. E., Kirby, C. W., and Stillman, M. J. (2008) Metal exchange in metallothioneins − a novel structurally significant Cd_5 species in the alpha domain of human metallothionein 1a. *FEBS J. 275*, 2227−2239.
(49) Palumaa, P., Tammiste, I., Kruusel, K., Kangur, L., Jörnvall, H., and Sillard, R. (2005) Metal binding of metallothionein-3 versus metallothionein-2: Lower affinity and higher plasticity. *Biochim. Biophys. Acta, Proteins Proteomics 1747*, 205−211.
(50) Petering, D. H., and Shaw, F. C., III (1991) Stability constants and related equilibrium properties of metallothioneins. In *Methods in Enzymology* (James, F., and Riordan, B. L. V., Eds.) pp 475−484, Academic Press, San Diego.
(51) Jacob, C., Maret, W., and Vallee, B. L. (1998) Control of zinc transfer between thionein, metallothionein, and zinc proteins. *Proc. Natl. Acad. Sci. U. S. A. 95*, 3489−3494.
(52) Cols, N., Romero-Isart, N., Capdevila, M., Oliva, B., Gonzàlez-Duarte, P., Gonzàlez-Duarte, R., and Atrian, S. (1997) Binding of excess cadmium (II) to Cd_7-metallothionein from recombinant mouse Zn_7-metallothionein 1. UV-VIS absorption and circular dichroism studies and theoretical location approach by surface accessibility analysis. *J. Inorg. Biochem. 68*, 157−166.
(53) Jiang, L.-J., Vašák, M., Vallee, B. L., and Maret, W. (2000) Zinc transfer potentials of the α- and β-clusters of metallothionein are affected by domain interactions in the whole molecule. *Proc. Natl. Acad. Sci. U. S. A. 97*, 2503−2508.
(54) Zalewska, M., Trefon, J., and Milnerowicz, H. (2014) The role of metallothionein interactions with other proteins. *Proteomics 14*, 1343−1356.
(55) Petering, D. H., Zhu, J., Krezoski, S., Meeusen, J., Kiekenbush, C., Krull, S., Specher, T., and Dughish, M. (2006) Apo-metallothionein emerging as a major player in the cellular activities of metallothionein. *Exp. Biol. Med. 231*, 1528−1534.
(56) Nielson, K. B., and Winge, D. R. (1985) Independence of the domains of metallothionein in metal binding. *J. Biol. Chem. 260*, 8698−8701.
(57) Ngu, T. T., and Stillman, M. J. (2006) Arsenic binding to human metallothionein. *J. Am. Chem. Soc. 128*, 12473−12483.
(58) Chen, S.-H., Russell, W. K., and Russell, D. H. (2013) Combining chemical labeling, bottom-up and top-down ion-mobility mass spectrometry to identify metal-binding sites of partially metalated metallothionein. *Anal. Chem. 85*, 3229−3237.
(59) Ngu, T. T., Dryden, M. D. M., and Stillman, M. J. (2010) Arsenic transfer between metallothionein proteins at physiological pH. *Biochem. Biophys. Res. Commun. 401*, 69−74.
(60) Palacios, Ò., Pagani, A., Pérez-Rafael, S., Egg, M., Höckner, M., Brandstätter, A., Capdevila, M., Atrian, S., and Dallinger, R. (2011) Shaping mechanisms of metal specificity in a family of metazoan metallothioneins: evolutionary differentiation of mollusc metallothioneins. *BMC Biol. 9*, 4.

DOI: 10.1021/acs.biochem.5b00452
Biochemistry 2015, 54, 5006−5016